Theory of half-metallic double perovskites. II. Effective spin Hamiltonian and disorder effects

Onur Erten,[1] O. Nganba Meetei,[1] Anamitra Mukherjee,[1,2] Mohit Randeria,[1] Nandini Trivedi,[1] and Patrick Woodward[3]
[1]*Department of Physics, The Ohio State University, Columbus, Ohio 43210, USA*
[2]*Department of Physics and Astronomy, University of British Columbia, Vancouver, BC V6T 1Z1, Canada*
[3]*Department of Chemistry, The Ohio State University, Columbus, Ohio 43210, USA*
(Received 31 October 2012; published 4 April 2013)

Double perovskites such as Sr_2FeMoO_6 are materials with half-metallic ground states and ferrimagnetic T_c's well above room temperature. This paper is the second of our comprehensive theory for half-metallic double perovskites. Here we derive an effective Hamiltonian for the Fe core spins by "integrating out" the itinerant Mo electrons and obtain an unusual double-square-root form of the spin-spin interaction. We validate the classical spin Hamiltonian by comparing its results with those of the full quantum treatment presented in a companion paper [O. N. Meetei *et al.*, Phys. Rev. B **87**, 165104 (2013)]. We then use the effective Hamiltonian to compute magnetic properties as a function of temperature and disorder and discuss the effect of excess Mo, excess Fe, and antisite disorder on the magnetization and T_c. We conclude with a proposal to increase T_c without sacrificing carrier polarization.

DOI: 10.1103/PhysRevB.87.165105 PACS number(s): 75.47.Lx, 72.80.Ga, 75.10.−b, 75.50.Gg

Strong electron correlations and the interplay among charge, spin, and lattice degrees of freedom lead to a wide range of spectacular phenomena in transition-metal oxides[1] such as high-T_c superconductivity, colossal magnetoresistance, and large thermopower.

Half metals with fully spin polarized ground states provide another example of such unique and spectacular phenomena. Among the known examples, double perovskites (DPs) are of particular interest due to their high ferromagnetic T_c's along with the possibility of integrating different functionalities with oxide electronics.[2] One of the best-studied half-metallic DPs is Sr_2FeMoO_6 (SFMO) with $T_c = 420$ K, well above room temperature.[2–4] DPs have the form $A_2BB'O_6$, which is derived from the simple ABO_3 perovskite structure with a three-dimensional (3D) checkerboard ordering of B and B' ions. DPs have a range of fascinating properties from spin liquids to multiferroics, as well as from metals to multiband Mott insulators.[2,3,5–7]

This article is the second part of our comprehensive theory for half-metallic double perovskites. Along with its companion paper[8] (hereafter referred to as paper I), it is an extension of our recent Letter.[9] We begin by summarizing the first paper where we discuss the full quantum Hamiltonian describing core spins on Fe coupled to conduction electrons through a generalized double-exchange mechanism. We calculated the magnetic and electronic properties as a function of temperature using exact diagonalization of the "fast" electronic degrees coupled to "slow" core spin configurations generated by classical Monte Carlo simulations (ED + MC). By retaining the electronic degrees of freedom, we obtained information about the temperature-dependent density of states and the destruction of the fully polarized half-metallic ground state through thermal fluctuations. One of our central results is that the conduction electron polarization at the chemical potential is directly proportional to the core-spin magnetization. This finding is significant because it indicates that if one can derive an effective Hamiltonian for the core spins, it would be possible to deduce the electronic polarization, a quantity of central importance for spin injection and spin transport, but one that is difficult to measure directly. The effective Hamiltonian also has the advantage that it can be used to simulate large system sizes compared to severe size limitations faced by ED + MC methods.

With this motivation, here we focus on describing the properties of the Fe core spins by "integrating out" the itinerant Mo electrons. The main results are as follows: (1) We derive a new effective Hamiltonian, $H_{\rm eff}$, for the classical spins by generalizing, in a nontrivial way, the Anderson-Hasegawa analysis for manganites[10] to double perovskites. The functional form of $H_{\rm eff}$ is different from standard Heisenberg or Anderson-Hasegawa Hamiltonians. (2) We validate $H_{\rm eff}$ by comparing its spin wave dispersion and temperature-dependent magnetization $M(T)$ with that of the full Hamiltonian obtained from the ED + MC method. $H_{\rm eff}$ indeed captures the magnetic properties of the full Hamiltonian at all temperatures whereas the Heisenberg Hamiltonian can only describe the low-temperature behavior. (3) We have performed the first 3D finite-temperature calculations of magnetic properties of DPs with accurate estimates of T_c using finite-size scaling. (4) The effective Hamiltonian also allows us to efficiently study the effects of disorder on $M(T)$. While both excess Fe and Mo decrease the saturation magnetization and T_c, antisite disorder, in which Fe and Mo exchange places, behaves differently; although magnetization drops, T_c is not affected. (5) The previous result forms the basis of our proposal to increase T_c without sacrificing conduction electron polarization. We propose that putting excess Fe and compensating the loss of carriers with La doping can indeed lead to a dramatic increase in T_c.

We start by briefly describing the full quantum Hamiltonian. We then solve the problem of two unit cells and derive the effective exchange Hamiltonian between two Fe core spins and generalize this form to the infinite lattice.

For large Hund's coupling $J_{\rm H}$, Fe^{3+} in the $3d^5$ configuration saturates the "up" manifold and forms a large spin $S = 5/2$ that we treat classically with a local axis of quantization along $\mathbf{S}_i$. Mo^{5+} ($4d^1$) contributes to conduction in t_{2g} orbitals. Due to the symmetry of t_{2g} orbitals, $d_{\alpha\beta}$ orbitals can only delocalize

in $\alpha\beta$ planes[11] ($\alpha\beta = xy, yz, xz$). For all the Mo sites j, we choose the same (global) axis of quantization. The generalized double-exchange Hamiltonian[9,12–15] that describes the core spins interacting with conduction electrons is

$$H = -t \sum_{\langle i,j\rangle,\sigma} (\epsilon_{i\sigma} d^{\dagger}_{i\downarrow} c_{j\sigma} + \text{H.c.}) - t' \sum_{\langle j,j'\rangle,\sigma} c^{\dagger}_{j\sigma} c_{j'\sigma} + \Delta \sum_{i} d^{\dagger}_{i\downarrow} d_{i\downarrow}, \quad (1)$$

where $d_{i\sigma}$ ($c_{i\sigma}$) are fermion operators on the Fe (Mo) sites with spin σ. The orientation (θ_i, ϕ_i) of the classical spins $\mathbf{S}_i$ affects the Mo-Fe hopping via $\epsilon_{i\uparrow} = -\sin(\theta_i/2)\exp(i\phi_i/2)$ and $\epsilon_{i\downarrow} = \cos(\theta_i/2)\exp(-i\phi_i/2)$.

I. EXACT SOLUTION OF TWO-SITE PROBLEM

We solve the Hamiltonian in Eq. (1) exactly analytically for two unit cells, shown schematically in Fig. 1. This is a generalization of the Anderson and Hasegawa analysis for manganites[10] applied to double perovskites.

In a single unit cell, there are three states derived from the $\text{Fe}_{\downarrow}$ and $\text{Mo}_{\uparrow,\downarrow}$ t_{2g} orbitals. We label the unit cells as i and j, and without loss of generality choose a coordinate system such that one of the core spins $\mathbf{S}_i$ is aligned with the z axis, and the other core spin $\mathbf{S}_j$ lies in the x-z plane [Fig. 1(a)]. This particular choice of coordinates simplifies the calculation as it gauges away the ϕ dependence. Thus, $\epsilon_{\uparrow} = \sin(\theta_i/2)$ and $\epsilon_{\downarrow} = \cos(\theta_i/2)$, where θ is the relative angle between $\mathbf{S}_i$ and $\mathbf{S}_j$. The two-unit-cell Hamiltonian is given by

$$H = \begin{pmatrix} \Delta & 0 & -t & 0 & 0 & -\gamma t \\ 0 & 0 & 0 & -\sin(\theta/2)t & 0 & 0 \\ -t & 0 & 0 & -\cos(\theta/2)t & 0 & 0 \\ 0 & -\sin(\theta/2)t & -\cos(\theta/2)t & \Delta & t\sin(\theta/2) & -t\cos(\theta/2) \\ 0 & 0 & 0 & t\sin(\theta/2) & 0 & 0 \\ -\gamma t & 0 & 0 & -\cos(\theta/2)t & 0 & 0 \end{pmatrix} \quad (2)$$

in the basis of $\{\text{Fe}_{i\downarrow}, \text{Mo}_{i\uparrow}, \text{Mo}_{i\downarrow}, \text{Fe}_{j\downarrow}, \text{Mo}_{j\uparrow}, \text{Mo}_{j\downarrow}\}$. Here $\gamma = 1$ for nearest-neighbor (NN) and 0 for next-nearest-neighbor (NNN) configurations [see Fig. 1(b)]. By converting the 6×6 matrix for H in a block diagonal form, it can be solved analytically. The eigenvalues are only a function of the angle between the core spins $\mathbf{S}_i$ and $\mathbf{S}_j$ and describe the effective magnetic exchange Hamiltonians. For the nearest-neighbor configuration ($\gamma = 1$), the lowest eigenvalue, describing one electron in two unit cells which corresponds to an electronic density of $n = 0.5$, is

$$H^{\text{FM}}_{\text{eff}} = -\sqrt{(\Delta/2)^2 + 2t^2[1 + \cos(\theta/2)]} \quad (3)$$

or equivalently

$$H^{\text{FM}}_{\text{eff}} = -\sqrt{(\Delta/2)^2 + 2t^2[1 + \sqrt{(1 + \mathbf{S}_i \cdot \mathbf{S}_j)/2}]}, \quad (4)$$

where $\mathbf{S}$ is the unit spin vector. We obtain a very interesting modified functional form with a double-square-root structure (see Fig. 2) that is different from conventional Heisenberg or previously studied Anderson-Hasegawa models.[10] Note that

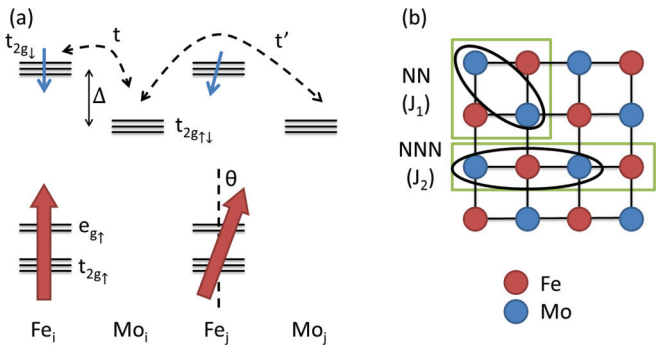

FIG. 1. (Color online) (a) Schematic showing energy levels at transition-metal sites in two unit cells (formula units) of SFMO. The Fe sites have localized $S = 5/2$ core spins, treated as classical vectors with orientation (θ, ϕ). The parameters t, t', and Δ of the Hamiltonian, Eq. (1), governing the dynamics of the itinerant electrons in t_{2g} orbitals, are also shown. (b) Nearest-neighbor (NN) and next-nearest-neighbor (NNN) configuration of two unit cells of DPs.

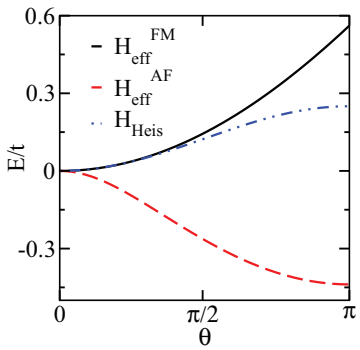

FIG. 2. (Color online) Energy as a function of θ for ferromagnetic H_{eff} (one electron in two unit cells) and antiferromagnetic H_{eff} (two electrons in two unit cells). Effective Hamiltonian gives hints for filling dependent magnetic phase transition. We include FM Heisenberg Hamiltonian (H_{Heis}) for comparison. Note that FM H_{eff} is quadratic for a broader range of θ compared to H_{Heis}.

the interaction is ferromagnetic with spin stiffness $J_{FM} \equiv \partial^2 E/\partial\theta^2$ obtained by expanding the energy close to $\theta = 0$, where $E(\theta) \approx E(0) + (1/2)(\partial^2 E/\partial\theta^2)\theta^2 + \mathcal{O}(\theta^4)$. We find

$$J_{FM} \sim \begin{cases} -t & \text{for} \quad t \gg |\Delta|, \\ -t^2/\Delta & \text{for} \quad t \ll |\Delta|, \end{cases} \tag{5}$$

showing that the kinetic energy of the conduction electrons sets the scale of the ferromagnetic exchange.

For two electrons in two unit cells, which corresponds to $n = 1$, the effective Hamiltonian is obtained by adding up the lowest two eigenvalues. For the NN configuration, the effective Hamiltonian is antiferromagnetic given by

$$H_{\text{eff}}^{\text{AF}} = -\sqrt{(\Delta/2)^2 + 2t^2[1 + \cos(\theta/2)]} - \sqrt{(\Delta/2)^2 + 2t^2[1 - \cos(\theta/2)]}. \tag{6}$$

Upon increasing the electron density ($n = 0.5 \to 1$), we find that the effective magnetic coupling changes from ferromagnetic to antiferromagnetic which is rather unconventional. Metallic antiferromagnetism with large local moments at a commensurate wave vector is rare in nature. Even at a two-unit-cell level, H_{eff} provides a hint for this transition and illuminates the mechanism, though only discrete fillings are accessible at this level. The filling-driven FM-AFM transition has also been discussed by others.[13] The exchange stiffness is given by

$$J_{AF} \sim \begin{cases} t & \text{for} \quad t \gg |\Delta|, \\ t^4/|\Delta^3| & \text{for} \quad t \ll |\Delta|, \end{cases} \tag{7}$$

with the scale for antiferromagnetism also set by the kinetic energy of the conduction electrons.

As we will discuss in the following section, SFMO with a conduction electron density $n = 0.33$ is far from any antiferromagnetic instability. We therefore consider only the ferromagnetic form of the two spin interaction. For convenience, we define two functions $F_1(x)$ and $F_2(x)$ that capture the NN and NNN ferromagnetic interactions respectively:

$$F_1(x) = 8\sqrt{2 + \sqrt{2 + 2x}} \tag{8}$$

and

$$F_2(x) = (5 + \sqrt{5})\sqrt{6 + 2\sqrt{3 + 2x}}, \tag{9}$$

where $x = \mathbf{S}_i \cdot \mathbf{S}_j$. Up to a constant factor of 8, $F_1(x)$ is obtained by setting $\Delta = 0$ (see Appendix) in Eq. (4). A similar procedure for the NNN exchange with γ set to zero in Eq. (2) yields $F_2(x)$.

II. EFFECTIVE SPIN HAMILTONIAN

Here we extend the analysis of *ferromagnetic* two-spin interaction discussed in the previous section to a full lattice in order to study the magnetic properties of SFMO. The effective spin Hamiltonian with NN and NNN interactions has the form

$$H_{\text{eff}} = -J_1 \sum_{\langle i,j \rangle} F_1(\mathbf{S}_i \cdot \mathbf{S}_j) - J_2 \sum_{\langle\langle i,j \rangle\rangle} F_2(\mathbf{S}_i \cdot \mathbf{S}_j), \tag{10}$$

where $F_1(x)$ and $F_2(x)$ are defined in Eqs. (8) and (9), respectively, and $x = \mathbf{S}_i \cdot \mathbf{S}_j$.

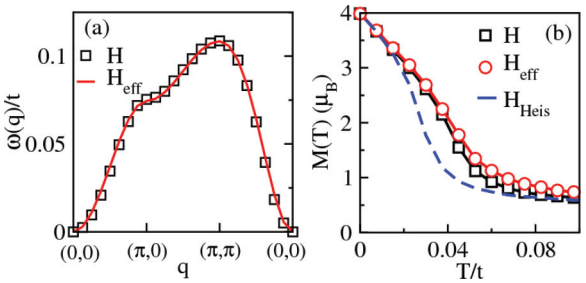

FIG. 3. (Color online) (a) Spin wave spectrum of full Hamiltonian and the H_{eff}. (b) $M(T)$ comparison between full Hamiltonian, H_{eff}, and Heisenberg Hamiltonian. All simulations are done with an 8×8 system due to the high computational cost of the exact diagonalization and Monte Carlo calculations.

We justify this Hamiltonian in two steps. First, we fix the values of J_1 and J_2 by matching the spin wave dispersion of H_{eff} with that of the full quantum Hamiltonian H [Eq. (1)]. In the second step, we compare the magnetization as a function of temperature, $M(T)$, obtained from H_{eff} and H. In the details described below, we show that our effective Hamiltonian completely describes the magnetic properties of SFMO at all temperatures.

For small θ, $F_{1(2)}(\cos\theta) \approx \text{const.} + (1/2)\theta^2$, which is the same as that of the Heisenberg interaction. The particular choice of prefactors [8 for F_1 and $(5 + \sqrt{5})$ for F_2] allows this simple comparison. It is therefore not surprising that the spin wave spectrum obtained by expanding H_{eff} around the FM ground state for small-angle deviations is the same as the Heisenberg model with NN and NNN interactions. As shown in Fig. 3(a), we can match the spin wave spectrum of the full quantum Hamiltonian with that of H_{eff} by tuning J_1 and J_2. This gives us the required values of J_1 and J_2 in our model. The agreement over the entire spectral range, rather than just at small energies, is indeed remarkable. We also point out that for the full quantum H we have used $\Delta = 2.5t$ and $t' = 0.1t$; however, the effective spin Hamiltonian is relatively insensitive to the value of Δ (see Appendix) and at the level of spin waves, the effects of Δ and t' are captured through J_1 and J_2. This justifies the simplifying assumption of $\Delta = 0$ used to obtain $F_{1(2)}(x)$.

For the second step of validating H_{eff}, we perform ED + MC calculations for the full quantum Hamiltonian along with classical Monte Carlo simulations for H_{eff} and for the Heisenberg Hamiltonian. In Fig. 3(b) we present a comparison of the temperature-dependent magnetization $M(T)$ calculated for each of these three Hamiltonians on an 8×8 system. It is remarkable to observe that $M(T)$ calculated from H_{eff} agrees remarkably well with that obtained for the full Hamiltonian *at all temperatures* thereby validating H_{eff}. Note that the Heisenberg Hamiltonian is only able to explain $M(T)$ at low temperatures and fails at intermediate temperatures $T \simeq T_c/2$.

Note that the full quantum model with classical spins coupled to conduction electrons has low-lying fermionic excitations. From a functional integral description, integrating out the fermions would give rise to various extra exchange terms like longer range interactions and four or more spin exchanges. The fact that we can reproduce $M(T)$ using H_{eff} at all temperatures shows that the effect of such terms is

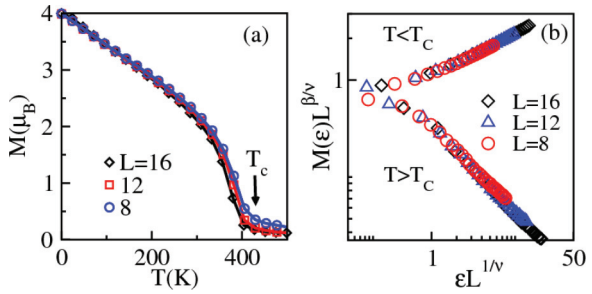

FIG. 4. (Color online) (a) Magnetization as a function of temperature, $M(T)$, of H_{eff} by classical Monte Carlo calculations for increasing 3D system sizes: 8^3, 12^3, and 16^3. (b) Estimating the thermodynamic T_c using finite-size scaling. $M(T)$ for different system sizes collapses to a universal function close to T_c with universal critical exponents. We used 3D O(3) universality class exponents and $\epsilon = |T - T_c|/T_c$ is the reduced temperature. As a result, we found $T_c = 0.14t$ for SFMO.

negligible and we indeed capture the most important magnetic exchange interactions within our model.

The agreement between $M(T)$ for H_{eff} and the full quantum Hamiltonian also indicates that both J_1 and J_2 are temperature independent. Although it is not clear *a priori* why this is the case, the fact that T_c is much less than the bandwidth provides a reasonable justification for the temperature independence of the exchange constants up to temperatures of order T_c.

Phase transition and determination of T_c. The primary advantage of the classical Hamiltonian H_{eff} is our ability to simulate much larger system sizes compared to those using ED + MC methods. We have performed the first 3D finite-temperature simulations of magnetic properties using classical Monte Carlo on up to 16^3 unit cells on an fcc lattice, as shown in Fig. 4(a). We have determined T_c using the finite-size scaling of $M(T)$. According to the finite-size scaling hypothesis, $M(T)$ for a system of size L^3 is described by a function of the form $M(T,L) = L^{-\beta/\nu}\mathcal{F}(\epsilon L^{1/\nu})$ where $\mathcal{F}(x)$ is a universal function and $\epsilon = |T - T_c|/T_c$. The critical exponents $\beta = 0.36$ and $\nu = 0.70$ are known for the 3D O(3) universality class. Using T_c as a fitting parameter, we plot $M(\epsilon)L^{\beta/\nu}$ against $\epsilon L^{1/\nu}$ for $L = 8$, 12, and 16. For the true thermodynamic T_c all curves, of different system sizes, collapse onto a single curve, as shown in Fig. 4(b) providing an estimate of $T_c = 0.14t$ for SFMO. Comparing with the experimental $T_c = 420$ K gives $t = 0.27$ eV which is in good agreement with electronic structure calculations.[4]

Low-temperature spin wave contribution to $M(T)$. Standard ferromagnetic spin waves produce a $T^{3/2}$ reduction of the magnetization, also known as the Bloch $T^{3/2}$ law.[16] However, in Fig. 3(c), $M(T)$ is linear at low T and this linear behavior in fact persists up to a relatively large fraction of T_c. We explain this difference between the Bloch law and the calculated linear behavior as arising from the difference between classical and quantum magnons. The classical Hamiltonian is equivalent to taking the $S \to \infty$ limit of the quantum Hamiltonian but keeping $T_c \sim JS^2$ constant. The $T^{3/2}$ law is restricted to a temperature scale $T_0 \lesssim T_c/S$, the magnon bandwidth, or equivalently to $T_0/T_c \sim 1/S$. Therefore the range of temperatures to observe the Bloch law is completely quenched in classical calculations and highly suppressed in the experiment due to the large $S = 5/2$ on Fe.

In order to understand the origin of the linear temperature dependence of the magnetization, we consider the reduction in $M(T)$ due to spin waves described by

$$M(T) = M_0\left[1 - \int_{1^{\text{st}}\text{B.Z.}} \frac{d^3q}{e^{\beta JSw_q} - 1}\right], \qquad (11)$$

where the integral is over the first Brillouin zone. For small q, the dispersion for magnons $w_q \sim q^2$. As $S \to \infty$ the exponential can be expanded at all temperatures: $e^{\beta JSw_q} = e^{\beta T_c w_q/S} \approx 1 + \frac{\beta T_c w_q}{S}$ for a constant T_c. Using this expansion and evaluating the integral gives $M(T) \sim M_0(1 - \alpha T)$ where $\alpha = \mathcal{O}(1)$. Thus classical spin waves indeed provide a natural explanation of the linear T dependence of the magnetization at low T.

The reason for the robustness of the linear $M(T)$ dependence up to relatively high temperatures is the peculiar double-square-root form of H_{eff} (see Fig. 2). Compared to the Heisenberg Hamiltonian, H_{eff} is harmonic ($E \sim J\theta^2$) for a larger domain of θ. Therefore magnon-magnon scattering which is mainly due to the nonharmonic part of the Hamiltonian is highly suppressed and that explains why the spin wave regime and correspondingly the linear T behavior of $M(T)$ survives up to relatively high T. Similar $M(T)$ has been observed in experiments both on single crystals[17] and on thin films.[18]

III. DISORDER

In SFMO, there are three common types of disorder: excess Fe, excess Mo, and antisite disorder (see Fig. 5). By using H_{eff}, we perform large-scale calculations of the temperature-dependent magnetic properties on systems up to 16^3 to investigate the effects of disorder. Finite-size effects close to T_c are highly suppressed with increasing system size as shown in Fig. 4(a). We start the discussion with the general chemical formula $Sr_2Fe_{1+y}Mo_{1-y}O_6$ with y greater (smaller) than zero corresponding to excess Fe (Mo), followed

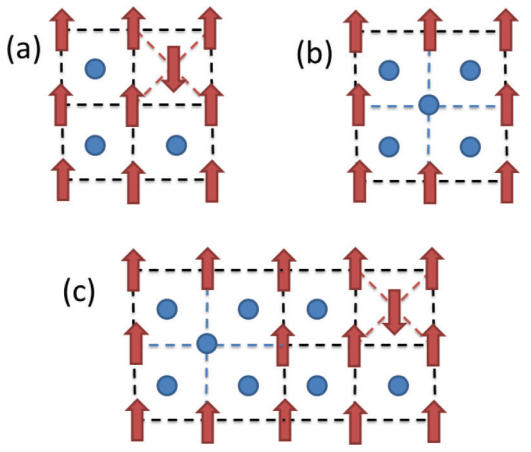

FIG. 5. (Color online) Types of disorder: (a) excess Fe, (b) excess Mo, (c) antisite disorder. Black, blue, and red lines represent FM bonds, the broken FM bonds, and the superexchange between Fe sites.

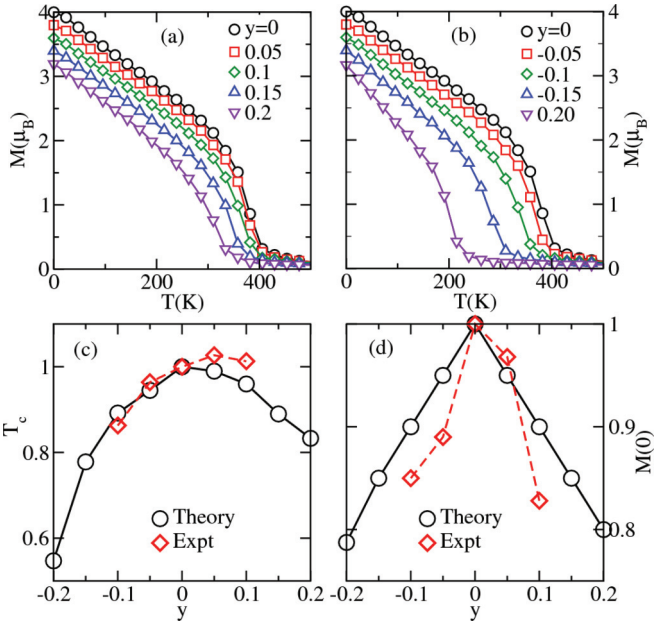

FIG. 6. (Color online) Effects of Fe and Mo disorder for $Sr_2Fe_{1+y}Mo_{1-y}O_6$ using H_{eff} and comparing it with experiments. (a) Fe-rich ($y > 0$) $M(T)$, (b) Mo-rich ($y < 0$) $M(T)$, (c) T_c as a function of y, (d) saturation magnetization, $M(0)$, with y compared with experiments (Ref. 19).

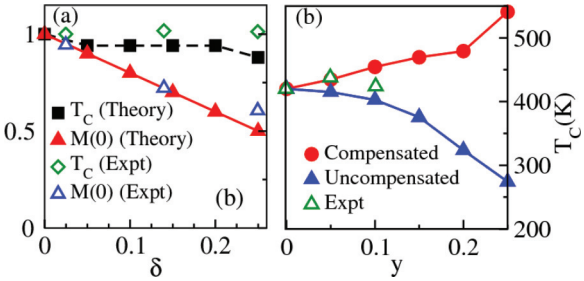

FIG. 7. (Color online) (a) Antisite disorder results for T_c and saturation magnetization, $M(0)$ (both normalized with respect to their disorder-free values) compared with experiments. (b) Proposal to increase T_c by La and Fe doping, $La_xSr_{2-x}Fe_{1+y}Mo_{1-y}O_6$. $T_c(y)$ for compensated ($x = 3y$) and uncompensated ($x = 0$). The uncompensated $T_c(y)$ is compared with experiments (Ref. 19).

by antisite disorder. We conclude with a proposal to increase T_c without sacrificing conduction electron polarization.

Excess Fe. For $y > 0$, as seen in Fig. 5(a) Fe replaces Mo sites which has two main effects: First, it reduces the total conduction electron density that weakens the double-exchange mechanism. Second, when two Fe sites are close to each other, the strong antiferromagnetic superexchange locks the spins. We estimate the strength of this superexchange $S(S+1)J_{\text{AF}} \sim 34$ meV based on $T_{\text{N}} = 750$ K for a similar compound $LaFeO_3$ with $S = 5/2$ spins on Fe. The excess Fe spin with the down orientation on the Mo site couples antiferromagnetically to the four neighboring up spins creating a local puddle that *enhances* ferromagnetism in its neighborhood. Capitalizing on this enhanced ferromagnetism will form the basis of our proposal to enhance T_c.

Figure 6(a) shows that the saturation magnetization $M(0)$ drops with increasing amount of excess Fe, largely because of its antiferromagnetic coupling to the neighboring Fe sites [see Fig. 6(d)]. For small values of y, T_c does not change significantly, then drops rapidly [Fig. 6(c)] beyond $y \simeq 0.1$. The initial insensitivity of T_c on y can be attributed to the two effects of excess Fe canceling each other: (1) Reduction of conduction electrons weakens FM, and (2) formation of ferromagnetic puddles locally stabilizes FM. The behavior of both $M(0)$ and T_c as a function of y is in good agreement with experiments.[19,20]

Excess Mo. Excess Mo ($y < 0$) leads to a dilution of the ferromagnetic bonds (see Fig. 5) as well as an increase in conduction electron density. The detrimental effects of dilution and broken ferromagnetic bonds on the magnetization as a function of T are shown in Fig. 6(b) and reflected directly in the rapid decrease of saturation magnetization $M(0)$ and T_c as a function of y [see Fig. 6(d)]. Once again these results are in good agreement with experiments.[19] The behavior of $M(0)$ in off-stoichiometric SFMO is also in agreement with DFT calculations.[21]

Antisite disorder. A realization of antisite disorder (AS) in which Fe and Mo sites replace each other is shown in Fig. 5(c). This is the most prevalent type of disorder in SFMO. It can be thought of as a combination of excess Fe and Mo disorder while keeping the carrier density constant. We quantify AS disorder using δ the fraction of Fe atoms that are on the Mo sublattice; $\delta = 0.5$ is a fully disordered system. Figure 7(a) shows that $M(0)$ drops linearly with a slope of $(1 - 2\delta)$, primarily due to the Fe spin on the wrong sublattice flipping from the parallel to the antiparallel direction, as shown in Fig. 5(c). T_c appears to be insensitive to AS disorder, primarily because two effects balance each other. While the broken FM bonds in the Mo-rich regions weaken FM, the puddles of Fe-rich regions have the opposite effect. Although Fe sites are coupled antiferromagnetically in these puddles, it locally creates stronger ferromagnetic domains. We believe that these two effects balance each other and T_c does not change significantly with antisite disorder, again in very good agreement with experiments.[19]

Proposal to increase T_c. We conclude with a proposal to increase T_c without sacrificing conduction electron polarization. We propose adding excess Fe, that locally creates strong ferromagnetic puddles, and simultaneously adding extra La to compensate the loss of carriers. Our results are shown in Fig. 7(b) and suggest that with adequate amount of La doping, T_c can be increased by about 100 K.

The general formula for both La and Fe doping is $La_xSr_{2-x}Fe_{1+y}Mo_{1-y}O_6$. Assuming that the Fe valency remains fixed at +3, and only Mo valency changes from +5 to $+5+\eta$ with doping, the charge balance dictates that $\eta = (2y - x)/(1 - y)$. The corresponding carrier concentration is $n = (1 + x - 3y)/3$. This implies that setting $y = 3x$ exactly compensates the lost carriers due to excess Fe and fixes the filling at $n = 1/3$. The dependence of T_c on excess Fe for the compensated case is shown in Fig. 7(b). We find that T_c increases by as much as 100 K for $y = 0.25$. Next we argue that our approach for enhancing T_c is better than only La doping. It is known that La substitution of $x = 1$ gives rise to a 15% increase of T_c.[22] However, this is accompanied by a huge increase in the extent of antisite

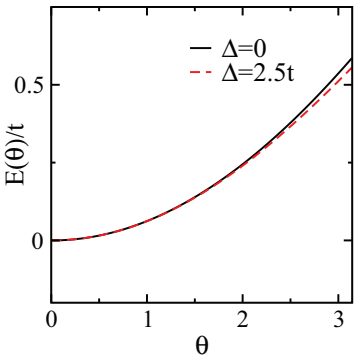

FIG. 8. (Color online) Comparison of energy as a function of θ for the two-site problem calculated using the spin Hamiltonian in Eq. (4) by setting $\Delta = 0$ (solid black) and $\Delta = 2.5$ (dashed red). They agree well for all values of θ.

disorder.[22] For $x = 1$, Mo valence changes from $+5$ to $+4$ (using $\eta = -x$). The reduced electrostatic attraction between the Mo and the surrounding oxygen octahedra leads to an expansion of the MoO_6 octahedra. As the volume of the MoO_6 octahedra approaches that of FeO_6, the B-B' ordering becomes fragile[2] and the increased antisite disorder reduces the polarization significantly.[8] In contrast, our proposal suggests a 25% increase in T_c is obtained for $y = 0.25$ and $x = 0.75$, with an average Mo valence of $+4.66$ which is unlikely to give rise to large amounts of antisite disorder.

Finally, we have checked that the proposed system with excess Fe and La compensation is indeed fully polarized at $T = 0$ using ED + MC. The increase in T_c by about 100 K is extremely encouraging as that would increase the room-temperature polarization significantly.

IV. CONCLUSION

We have found a nontrivial generalization of the double-exchange mechanism that is relevant for driving ferromagnetism in the double-perovskite half metals. The effective magnetic Hamiltonian H_{eff} with the double-square-root form, obtained after integrating out the itinerant electrons, is very different from standard Heisenberg or double-exchange Hamiltonians and agrees remarkably well when compared with the full quantum Hamiltonian. H_{eff} is found to retain the harmonic θ^2 form in the canting between neighboring spins up to a larger range of θ. As a result classical spin waves provide a good description of the temperature-dependent $M(T)$, with suppressed magnon-magnon scattering. We have performed large-scale simulations of H_{eff} with different types of disorder. From our insights on the dependence of the saturation magnetization and T_c on disorder, we propose a mechanism to substantially increase T_c by balancing excess Fe doping and compensating the loss of carriers with La doping.

ACKNOWLEDGMENTS

We thank D. D. Sarma for fruitful discussions. Funding for this research was provided by the Center for Emergent Materials at the Ohio State University, an NSF MRSEC (Award No. DMR-0820414).

APPENDIX: INCLUDING EFFECTS OF Δ IN H_{eff}

Here we show that the effects of Δ can be included in the spin Hamiltonian shown in Eq. (10) which we derived by setting $\Delta = 0$. As justified in the main text, for small deviations from the ferromagnetic ground state the spin wave dispersion has the Heisenberg form which can be captured by appropriately fitting the spin wave spectrum of H_{eff} to that of the full quantum Hamiltonian with $\Delta \neq 0$. There is, however, still the question of how well the model describes large spin canting which is the main focus of our work. In Fig. 8 we have shown the energy as a function of θ for the two-site problem calculated using the spin Hamiltonian in Eq. (4) by setting $\Delta = 0$ and $\Delta = 2.5$. It is clearly seen that once the spin stiffness is appropriately chosen to match the low-energy dispersion, the two models agree within a precision of less than 3% for all values of θ. This justifies our approach of using the simplest model with $\Delta = 0$.

[1] M. Imada, A. Fujimori, and Y. Tokura, Rev. Mod. Phys. **70**, 1039 (1998).
[2] D. Serrate, J. M. D. Teresa, and M. R. Ibarra, J. Phys.: Condens. Matter **19**, 023201 (2007).
[3] K.-I. Kobayashi, T. Kimura, H. Sawada, K. Terakura, and Y. Tokura, Nature (London) **395**, 677 (1998).
[4] D. D. Sarma, P. Mahadevan, T. Saha-Dasgupta, S. Ray, and A. Kumar, Phys. Rev. Lett. **85**, 2549 (2000).
[5] G. Chen, R. Pereira, and L. Balents, Phys. Rev. B **82**, 174440 (2010).
[6] G. Chen and L. Balents, Phys. Rev. B **84**, 094420 (2011).
[7] O. N. Meetei, O. Erten, M. Randeria, N. Trivedi, and P. Woodward, Phys. Rev. Lett. **110**, 087203 (2013).
[8] O. N. Meetei, O. Erten, A. Mukherjee, M. Randeria, N. Trivedi, and P. Woodward, Phys. Rev. B **87**, 165104 (2013).
[9] O. Erten, O. N. Meetei, A. Mukherjee, M. Randeria, N. Trivedi, and P. Woodward, Phys. Rev. Lett. **107**, 257201 (2011).
[10] P. W. Anderson and H. Hasegawa, Phys. Rev. **100**, 675 (1955).
[11] A. B. Harris, T. Yildirim, A. Aharony, O. Entin-Wohlman, and I. Y. Korenblit, Phys. Rev. B **69**, 035107 (2004).
[12] J. L. Alonso, L. A. Fernández, F. Guinea, F. Lesmes, and V. Martin-Mayor, Phys. Rev. B **67**, 214423 (2003).
[13] P. Sanyal and P. Majumdar, Phys. Rev. B **80**, 054411 (2009).
[14] A. A. Aligia, P. Petrone, J. O. Sofo, and B. Alascio, Phys. Rev. B **64**, 092414 (2001).
[15] P. Petrone and A. A. Aligia, Phys. Rev. B **66**, 104418 (2002).
[16] P. Fazekas, *Lecture Notes on Electron Correlation and Magnetism* (World Scientific, Singapore, 1999).
[17] Y. Tomioka, T. Okuda, Y. Okimoto, R. Kumai, K.-I. Kobayashi, and Y. Tokura, Phys. Rev. B **61**, 422 (2000).
[18] A. J. Hauser, R. E. A. Williams, R. A. Ricciardo, A. Genc, M. Dixit, J. M. Lucy, P. M. Woodward, H. L. Fraser, and F. Yang, Phys. Rev. B **83**, 014407 (2011).

[19]D. Topwal, D. D. Sarma, H. Kato, Y. Tokura, and M. Avignon, Phys. Rev. B **73**, 094419 (2006).
[20]K. Yoshida, S. Ikeuchi, H. Shimizu, S. Okayasu, and T. Suzuki, J. Phys. Soc. Jpn. **80**, 044716 (2011).
[21]R. Mishra, O. D. Restrepo, P. M. Woodward, and W. Windl, Chem. Mater. **22**, 6092 (2010).
[22]J. Navarro, C. Frontera, L. Balcells, B. Martinez, and J. Fontcuberta, Phys. Rev. B **64**, 092411 (2001).